Characterizing Tumor Invasiveness of Glioblastoma Using Multiparametric Magnetic Resonance Imaging

Chao Li, MD[1,2,3], Shuo Wang, BSc[4], Jiun-Lin Yan, MD PhD[1,5,6], Turid Torheim, PhD[7,8], Natalie R. Boonzaier, PhD[1,9], Rohitashwa Sinha, MRCS[1], Tomasz Matys, MD PhD[4,10], Florian Markowetz, PhD[7,8], and Stephen J. Price, PhD FRCS[1,11]

Corresponding author: Chao Li

Email: cl109@outlook.com

Address: Box 167 Cambridge Biomedical Campus, Cambridge, UK, CB2 0QQ

Phone: (44)7732924953; **FAX:** +44 (0)1223 216926

[1]Cambridge Brain Tumor Imaging Laboratory, Division of Neurosurgery, Department of Clinical Neurosciences, University of Cambridge, Cambridge, UK

[2]Department of Neurosurgery, Shanghai General Hospital (originally named "Shanghai First People's Hospital"), Shanghai Jiao Tong University School of Medicine, China

[3]EPSRC Centre for mathematical imaging in healthcare, University of Cambridge, Cambridge, UK

[4]Department of Radiology, University of Cambridge, Cambridge, UK

[5]Department of Neurosurgery, Chang Gung Memorial Hospital, Keelung, Taiwan;

[6]Chang Gung University College of Medicine, Taoyuan, Taiwan

[7]Cancer Research UK Cambridge Institute, University of Cambridge, Cambridge, UK

[8]CRUK & EPSRC Cancer Imaging Centre in Cambridge and Manchester, Cambridge, UK

[9]Developmental Imaging and Biophysics Section, Great Ormond Street Institute of Child Health, University College London, London, UK

[10]Cancer Trials Unit, Department of Oncology, Addenbrooke's Hospital, Cambridge, UK

[11]Wolfson Brain Imaging Centre, Department of Clinical Neurosciences, University of Cambridge, Cambridge, UK

Key Words: Glioblastoma; magnetic resonance imaging; diffusion tensor imaging; magnetic resonance spectroscopy; prognosis; oncology

Running Title: Characterizing Tumor Invasiveness of Glioblastoma

Abstract word count: 308; Text word count: 2721;

Number of references: 28; Number of tables and/or figures: 7

Ethics approval and consent to participate

Ethics Reference No.: 10/H0308/23; ISRCTN Registration No.: ISRCTN62033854

Written informed consent was obtained from all subjects (patients) in this study.

Funding

The research was supported by the National Institute for Health Research (NIHR) Brain Injury MedTech Co-operative based at Cambridge University Hospitals NHS Foundation Trust and University of Cambridge; The views expressed are those of the author(s) and not necessarily those of the NHS, the NIHR or the Department of Health and Social Care (SJP, project reference NIHR/CS/009/011); CRUK core grant C14303/A17197 and A19274 (FM lab); Cambridge Trust and China Scholarship Council (CL & SW); the Chang Gung Medical Foundation and Chang Gung Memorial Hospital, Keelung, Taiwan (JLY); CRUK & EPSRC Cancer Imaging Centre in Cambridge & Manchester (FM & TT, grant C197/A16465); NIHR Cambridge Biomedical Research Centre (TM & SJP); Commonwealth Scholarship Commission and Cambridge Commonwealth Trust (NRB).

Abstract

Objective

To characterize the abnormalities revealed by diffusion tensor imaging (DTI) using magnetic resonance spectroscopy and perfusion imaging, and to evaluate the prognostic value of a proposed quantitative measure of tumor invasiveness by combining contrast-enhancing and DTI abnormalities in glioblastoma patients.

Methods

Eighty-four glioblastoma patients were recruited pre-operatively. DTI was decomposed into isotropic (p) and anisotropic (q) components. The relative cerebral blood volume (rCBV) were calculated from the dynamic susceptibility contrast imaging. Values of N-acetyl aspartate (NAA), myoinositol (mIns), choline (Cho), lactate (Lac) and glutamate + glutamine (Glx) were measured from multivoxel magnetic resonance spectroscopy and normalized as ratios to creatine (Cr). Tumor regions of interest (ROIs) were manually segmented from the contrast-enhancing T1-weighted (CE-ROI) and DTI-q (q-ROI) maps. Perfusion and metabolic characteristics of above ROIs were measured and compared. Relative invasiveness coefficient (RIC) was calculated as a ratio of the characteristics radius of CE-ROI and q-ROI. The prognostic significance of RIC was tested using Kaplan-Meier and multivariate Cox regression analyses.

Results

The Cho/Cr, Lac/Cr and Glx/Cr in q-ROI were significantly higher than CE-ROI ($P = 0.004$, $P = 0.005$ and $P = 0.007$, respectively). CE-ROI had significantly higher rCBV values than q-ROI ($P < 0.001$). A higher RIC was associated with worse survival in multivariate overall survival (OS) model (hazard ratio [HR] = 1.40, 95% CI: 1.06-1.85, $P = 0.016$) and progression-free survival (PFS) model (HR = 1.55, 95% CI: 1.16-2.07, $P = 0.003$). An RIC cutoff value of 0.89 significantly predicted shorter OS (median 244 and 384 days, respectively; $P = 0.002$) and PFS (median 406 and 605 days, respectively; $P = 0.001$).

Conclusions

DTI-q abnormalities displayed higher tumor load and hypoxic signatures compared to contrast-enhancing abnormalities, whereas contrast enhancing regions potentially represented the proliferation front. Integrating the invasion extents of DTI-q and contrast enhancing volume into clinical practice may lead to improved treatment efficacy.

Introduction

Glioblastomas are the most common malignant brain tumors in adults, characterized by dismal patient survival. Although maximal safe resection followed by radiotherapy with concomitant and adjuvant temozolomide chemoradiotherapy has improved patient outcomes, the median overall survival remains 12-15 months.[1] Accumulating evidence suggests that aggressive surgical resection can prolong patient survival.[2, 3] However, extended surgical resection or escalating adjuvant radiation volume may subject the patient to a higher risk of neurologic deficits. A more accurate targeting of tumor with less risk of functional damage to patients is therefore crucial for treatment planning.

Magnetic resonance imaging (MRI) is widely used in monitoring the disease and defining tumor region. In current clinical practice, contrast-enhancing T1-weighted imaging is considered as the gold standard for planning surgery and radiotherapy. Glioblastoma is characterized by its infiltration into the surrounding brain tissue. Thus, infiltrative tumor cells are well known beyond the contrast-enhancing region.[4] Other conventional sequences, including T2-weighted and fluid-attenuated inversion recovery (FLAIR), are non-specific in differentiating tumour invasion from peritumoral edema and treatment effects that cause white matter change.[5]

Many MR methods have been developed that provide signals relating to pathological changes in the tumour.[6] Diffusion tensor imaging (DTI) measures the magnitude and direction of water mobility and is sensitive at detecting tumor invasion that leads to the disruption of brain microstructure.[7, 8] Previous work has shown that the diffusion tensor can be decomposed into isotropic (DTI-p) and anisotropic (DTI-q) components.[9] The resulting DTI-p and -q maps have potential in delineating tumor invasion.[4, 10] Image-guided biopsy studies have shown that DTI-q abnormalities represent regions of higher tumor burden.[4] A recent retrospective study revealed that more extensive resection of DTI-q and contrast-enhancing abnormalities was

associated with improved patient outcome, suggesting both abnormality areas could be clinically relevant.[11]

The first purpose of this study was to compare the pre-treatment DTI-q and contrast enhancing abnormalities using magnetic resonance spectroscopy and perfusion imaging in treatment naive patients. As DTI-q may represent a tumor region with high tumor load, we hypothesized that the DTI-q abnormality would represent a more hypoxic region resulting from the higher cellularity in this region. On the other hand, as the contrast-enhancement is associated with the contrast agent leakage, we hypothesized that the contrast-enhancing abnormality may represent a region with more evidence of neovascularization, indicated by the aberrant perfusion.

The second purpose of this study was to evaluate the prognostic value of a quantitative measure of tumour invasiveness, in which we integrated both volumes of DTI-q and contrast-enhancing abnormalities. Various studies have shown that hypoxia may be a factor driving tumor progression.[12] Further, angiogenesis can be activated by hypoxia through a series of proangiogenic factors, leading to neovascularization during tumor expansion.[13] Therefore, we hypothesized that combining both DTI-q and contrast-enhancing abnormalities could be of prognostic value.

Materials and Methods

Patient population

Patients with a suspected diagnosis of supratentorial newly diagnosed glioblastoma were prospectively recruited from July 2010 to August 2015. All patients were required to have a good performance status (World Health Organization performance status 0-1) before surgery. Patients who had a history of a previous brain tumor, cranial surgery, radiotherapy/chemotherapy, or contraindication for MRI scanning were excluded. This study was approved by the local institutional review board. Signed informed consent was obtained from each patient.

Treatment and response assessment

Neuronavigation (StealthStation, Medtronic) and 5-aminolevulinic acid fluorescence were used to guide surgery, with other adjuvants (e.g. cortical and subcortical mapping) to allow maximal safe resection when appropriate. Extent of resection was assessed according to the postoperative MRI within 72 hours, classified as either complete resection of enhancing tumor, partial resection of enhancing tumor or biopsy.[14] Patients' treatment response was evaluated according to the Response Assessment in Neuro-oncology criteria,[5] which incorporates clinical and radiological measurements for assessment. All MRI and histological data were collected prospectively. In some cases, pseudoprogression was suspected when new enhancement was observed within 12 weeks after radiotherapy. In these cases, patient's treatment was continued, and true progression or pseudoprogression was determined retrospectively.

Pre-operative MRI acquisition

All MRI sequences were performed on a 3-Tesla MRI system (Magnetron Trio; Siemens Healthcare, Erlangen, Germany) with a standard 12-channel receive-head coil[15]. MRI sequences were acquired as following: post-contrast T1-weighted sequence (TR/TE/TI 2300/2.98/900 ms; flip angle 9°; FOV 256 × 240 mm; 176-208 slices; no slice gap; voxel size

1.0 × 1.0 × 1.0 mm) after intravenous injection of 9 mL gadobutrol (Gadovist,1.0 mmol/mL; Bayer, Leverkusen, Germany); T2-weighted sequence (TR/TE 4840-5470/114 ms; refocusing pulse flip angle 150°; FOV 220 × 165 mm; 23-26 slices; 0.5 mm slice gap; voxel size of 0.7 × 0.7 × 5.0 mm); T2-weighted fluid attenuated inversion recovery (FLAIR) (TR/TE/TI 7840-8420/95/2500 ms; refocusing pulse flip angle 150°; FOV 250 × 200 mm; 27 slices; 1 mm slice gap; voxel size of 0.78125 × 0.78125 × 4.0 mm). PWI was acquired with a dynamic susceptibility contrast-enhancement (DSC) sequence (TR/TE 1500/30 ms; flip angle 90°; FOV 192 × 192 mm; 19 slices; slice gap 1.5 mm; voxel size of 2.0 × 2.0 × 5.0 mm;) with 9 mL gadobutrol (Gadovist 1.0 mmol/mL) followed by a 20 mL saline flush administered via a power injector at 5 mL/s. DTI was acquired before contrast imaging, using a single-shot echo-planar sequence (TR/TE 8300/98 ms; flip angle 90°; FOV 192 × 192 mm; 63 slices; no slice gap; voxel size 2.0 × 2.0 × 2.0 mm); Inline ADC calculation was performed during DTI acquisition from using b values of 0–1000 sec/mm^2. Multivoxel 2D ^{1}H-MRS chemical shift imaging (CSI) utilized a semi-LASER sequence (TR/TE 2000/30-35 ms; flip angle 90°; FOV 160 × 160 mm; voxel size 10 × 10 × 15-20 mm). PRESS excitation was selected to encompass a grid of 8 rows × 8 columns on T2-weighted images.

Imaging processing

All other sequences were co-registered to the T2-weighted images, which were used to plan the chemical shift imaging in each subject. The co-registration was performed using the linear image registration tool (FLIRT) functions in Oxford Centre for Functional MRI of the Brain (FMRIB) Software Library (FSL) v5.0.0 (Oxford, UK).[16] DSC processing and leakage correction was performed with the NordicICE software (NordicNeuroLab, Bergen, Norway), in which the arterial input function was automatically defined. The relative cerebral blood volume (rCBV) maps were calculated. DTI images were processed using the diffusion toolbox (FDT) in FSL,[17] during which normalization and eddy current correction were performed. The

decomposition of processed DTI images into isotropic component (p) and anisotropic component (q) was performed using a previously described method.[9]

Regions of interest

Tumor regions of interest (ROIs) were manually segmented on the co-registered contrast-enhancing (CE) T1-weighted and DTI-q images. The delineation was independently performed blinded to the outcome by the authors with fair agreement (Figure 1).[10, 11] To compare the imaging characteristics, a Boolean subtraction of CE and p abnormalities was performed in MATLAB (MathWorks, Inc., Natick MA) to obtain the CE-ROI (without DTI-q abnormality) and q-ROI.

For each individual subject, normal-appearing white matter (NAWM) regions were drawn manually in the contralateral white matter as normal controls. Each voxel value in the ROIs was normalized by dividing it by the mean voxel value of the contralateral normal-appearing white matter.

Tumor characteristic radius

To quantify the extent of irregular tumors in 3D space, the characteristic radius of ROIs were calculated using a previously reported method.[18] Briefly, the smallest bounding ellipsoid was fitted to the whole tumor volume revealed by ROIs. The length of this ellipsoid's semi-major axis was used to measure the characteristic radius of tumor ROI. We then calculated the ratio of CE characteristic radius to DTI-q characteristic radius, as a relative invasiveness coefficient (RIC). A demonstration of the calculation of characteristic radius and RIC is provided (Figure 2).

Multivoxel MRS processing

CSI data were processed using LCModel (Provencher, Oakville, Ontario)[15]. All the concentrations of metabolites were calculated as a ratio to creatine (Cr).[19] All relevant spectra from CSI voxels of interest were assessed for artefacts using previously described criteria.[20]

The values of the Cramer–Rao lower bounds were used to evaluate the quality and reliability of CSI data and values with standard deviation (SD) > 20% were discarded.[20]

To account for the difference in spatial resolution, all tumor pixels which have been co-registered to T2 space were projected to CSI space which were planned in T2 space, according to their coordinates using MATLAB. The proportion of T2-space tumor pixels occupying each CSI voxel was calculated. Only CSI voxels that were completely located within tumor ROIs were included for further analysis. The weight of each CSI voxel was taken as the proportion of the tumor pixels in that CSI voxel. The weighted sum value was used as the final metabolic value of the tumor ROIs.

Statistical analysis

All statistical analyses were performed in RStudio v3.2.3 (Boston, MA, USA). The CSI data and rCBV values were compared with pairwise Kruskal-Wallis rank sum test using Benjamini-Hochberg procedure to control the false discovery rate in multiple comparisons. Categorical variables were tested with chi-square test. The Kaplan-Meier and Cox proportional hazards regression analyses were performed to evaluate patient survival. In Kaplan-Meier analysis, RIC was dichotomized using the median value of all patients in the cohort. For Cox proportional hazards regression, all other relevant covariates, including IDH-1 mutation status, MGMT promoter methylation status, sex, age, extent of resection and contrast-enhancing volume were considered. Patients who were alive at the last known follow-up were censored. The hypothesis of no effect was rejected at a two-sided level of 0.05.

Results

Patients

A total of 136 patients were recruited. After surgery, twenty-one patients were excluded due to a non-glioblastoma pathology diagnosis. Due to their post-operative performance status, 84 of 115 (73.0%) patients received concurrent temozolomide chemoradiotherapy followed by adjuvant temozolomide (Stupp protocol). Other patients received short-course radiotherapy (17.4%, 20/115), or best supportive care (9.6%, 11/115), respectively. We only included the 84 patients who have received the Stupp protocol for final analysis. Survival data were available for 80 of 84 (95.2%) patients and four (4.8%) patients were lost to follow up. Patient clinical characteristics are summarized in Table 1.

Tumor volume and characteristic radius

The volumes of T1-weighted contrast-enhancement and DTI-q abnormalities are in Table 1. The characteristic radii (mean ± SD) of the contrast-enhancing tumor region and DTI-q abnormalities were 3.6 ± 0.8 cm and 3.2 ± 0.8 cm, respectively.

Imaging characteristics of tumor regions

In the comparison of rCBV, CE-ROI (2.52 ± 1.18, 95% CI: 2.25-2.80) had significantly higher rCBV values than q-ROI (2.08 ± 1.23, 95% CI: 1.85-2.30, $P < 0.001$). For MRS comparisons, both tumor ROIs displayed abnormal metabolic signatures, compared to the normal appearing white matter (all $P < 0.001$) (Figure 3). A full comparison is demonstrated in Supplementary Table 1.

Specifically, the Cho/Cr in q-ROI (0.66, 95% CI: 0.63-0.70) was significantly higher than CE-ROI (0.56, 95% CI: 0.54-0.59, $P = 0.004$). The Lac/Cr in q-ROI (7.79, 95% CI: 6.34-9.24) was significantly higher than CE-ROI (4.17, 95% CI: 3.49-4.85, $P = 0.005$). The Glx/Cr in q-ROI (2.60, 95% CI: 2.373-2.83) was significantly higher than CE-ROI (2.08, 95% CI: 1.94-2.22, $P = 0.007$).

Although not significant, the Cho/NAA ratio of q-ROI (0.84, 95% CI: 0.75-0.92) had a higher Cho/NAA ratio than CE-ROI (0.75, 95% CI: 0.63-0.87, $P = 0.055$). The mIns/Cr ratio of q-ROI (1.59, 95% CI: 1.44-1.73) was higher than CE-ROI (1.45, 95% CI: 1.33-1.56, $P = 0.085$). There was no significant difference between the NAA/Cr ratios of q-ROI (0.88, 95% CI: 0.83-0.93) and CE-ROI (0.91, 95% CI: 0.86-0.95, $P = 0.171$).

Patient outcomes

The prognostic value of RIC was tested in multivariate survival models. The model of OS showed extent of resection (HR = 2.32, 95% CI: 1.20-4.44, $P = 0.012$), the volume of CE (HR = 1.59, 95% CI: 1.20-2.29, $P = 0.007$) and RIC (HR = 1.40, 95% CI: 1.06-1.85, $P = 0.016$) significantly affected OS. In multivariate modelling of PFS, extent of resection (HR = 3.27, 95% CI: 1.67-6.38, $P < 0.001$), and RIC (HR = 1.55, 95% CI: 1.16-2.07, $P = 0.003$) significantly affected PFS.

We then dichotomized patients into 2 subgroups using the median value of RIC= 0.89, with 42 patients in each group. The subgroup with a RIC of greater than 0.89 had a significantly shorter survival than those with a RIC of less than 0.89 (for PFS: $P = 0.001$, for OS: $P = 0.002$) (Table2, Figure 4). No statistical difference was found between these 2 patient subgroups, in age, sex, extent of resection, pre-operative tumor volumes, MGMT promoter methylation and IDH-1 mutation status (Table 2). Two case examples with a RIC of less than 0.89 and a RIC of more than 0.89 are provided in Figure 5.

Discussion

In this study, we characterized contrast enhancing and DTI-q abnormalities using multiparametric MRI and evaluated a proposed coefficient in assessing tumor invasiveness, which was calculated from the characteristics radii of contrast enhancing and DTI-q abnormalities. The results showed that DTI-q abnormalities may represent a hypoxic tumor region. Integrating this coefficient into the survival model was useful in estimating tumor aggressiveness and predicting patient survivals.

DTI-q reveals tumor regions with abnormal metabolic signatures

Although providing useful structural information, conventional imaging is insufficient in reflecting tumor physiology.[4] The integration of advanced MRI technique into clinical practice has been recommended for improving tumor volume targeting. Various findings support that DTI is useful in revealing tumor invasion and predicting patient survival.[21, 22] In accordance with these studies, our current results of MR spectroscopy indicated that the q-ROI displayed abnormal metabolic signatures.

DTI-q and contrast enhancement represent different tumor properties

In our results, the DTI-q abnormality showed a higher Cho/Cr ratio than the contrast enhancing region, which implies that the DTI-q abnormality regions may have higher cellularity than contrast enhancing regions, as choline is regarded as a marker of cell membrane turnover.[23] The intensive tumor load in DTI-q abnormality may lead to hypoxia, which is supported by the significantly higher Lac/Cr level in DTI-q abnormality, compared to the contrast enhancing region and normal control. The significantly elevated level of Glx, compared to the contrast enhancing region, also suggested the neuronal destruction and hypoxic microenvironment in DTI-q abnormality region.[24, 25] Compared to DTI-q abnormality, contrast enhancing regions displayed a significantly elevated rCBV, which had a positive correlation with MIB-1 index in

a previous biopsy study.[26] This suggests that the contrast enhancing tumor may indicate a proliferative front of the tumor.

The relative invasiveness coefficient combines DTI-q and contrast-enhancing volumes

It is well known that hypoxia may be a driving force of tumor invasion and proliferation[12]. We hypothesized that the ratio of contrast-enhancing radius to DTI-q radius could indicate the tendency of tumor proliferation driven by hypoxia, which may can potentially quantify tumor invasiveness. We tested this coefficient in the survival model and found clinical relevance with patient outcomes. Specifically, higher RIC may indicate a more aggressive tumor phenotype, in which the leading edge of proliferation runs further beyond the hypoxic core. It was previously reported that combining T1-weighted and T2-weighted images is useful in quantifying tumor invasiveness.[27] Here we proposed our approach by integrating physiological imaging with structural imaging, which might potentially provide a more physiologically relevant measure.

Clinical implications and limitations

Our study may have neurosurgical implications. An extended extent of resection can significantly improve overall survival of the newly diagnosed glioblastoma.[28] The survival benefit from maximal safe resection is associated with not only extensive cytoreduction,[29] but also improvement of the efficacy of temozolomide regimen[3]. Multiparametric MRI can facilitate the characterization of the multifaceted tumor properties. Our findings showed that DTI-q is an invasive region and that integrating contrast-enhancing and DTI-q volume may have prognostic value. Although the average volumes of contrast-enhancing and DTI-q abnormalities are similar, their locations and morphology can be different. Particularly, for patients who have a greater extent of DTI-q abnormality than contrast-enhancing abnormality, a combination of both tumor areas into image-guided navigation may potentially bring benefits for maximal safe resection in surgical planning.

Our study had limitations. Firstly, the resolution of CSI was lower than anatomical imaging and ^{1}H MR spectroscopy voxels were larger than anatomical and physiological voxels. Secondly, our previous results have validated the imaging markers using histological assessment and longitudinal observations, further biological studies may be needed for future clinical application.

Conclusions

The imaging characteristics of DTI-q abnormality suggest that it is a hypoxic region with high tumor burden. Integrating the extent of DTI-q and contrast enhancing regions into clinical practice may bring benefits for patient care.

Table 1. Patient characteristics

Characteristics	Value
Total no. of patients	84
Male	62
Female	22
Age (years)	57.3 ± 10.7
Complete resection no. of patients	60
Partial resection no. of patients	22
Biopsy	2
MGMT methylation* positive no of patients (%)	37 (45.1 %)
IDH-1 mutation positive, no of patients (%)	7 (8.3 %)
Contrast-enhancing volumes, $cm^{3\#}$	44.2 ± 27.2
DTI-q abnormality volumes, $cm^{3\#}$	43.8 ± 27.1
Progression-free survival (days)	264 (25-1130)
Overall survival (days)	461 (52 -1376)

*MGMT methylation status unavailable for 2 patients; #mean ± SD. SD: standard deviation; MGMT: O-6-methylguanine-DNA methyltransferase; IDH-1: Isocitrate dehydrogenase 1; cm: centimeter; OS: overall survival; PFS: progression-free survival.

Table 2. Clinical characteristics of the patient subgroups

Characteristics	RIC > 0.89	RIC ≤ 0.89	*P* Value
Age (years)	58.1 ± 10.3	56.4 ± 11.1	0.661
Sex			
Male	33	29	0.457
Female	9	13	
Extent of resection (of enhancing tumor)			
Complete resection	29	30	0.883
Partial resection	12	10	
Biopsy	1	1	
MGMT promoter methylation status*			
Methylated	15	22	0.183
Unmethylated	26	19	
IDH-1 mutation status			
Mutant	2	5	0.430
Wild-type	40	37	
Pre-operative tumor volumes (cm3) #			
Contrast-enhancing	48.3 ± 28.0	40.0 ± 14.7	0.291
DTI-q	41.5 ± 27.4	46.1 ± 26.7	0.263
Survival (days)			
Median OS (range)	384 (52-839)	605 (25-1130)	**0 .002**[†]
Median PFS (range)	244 (37-550)	406 (135-1259)	**0 .001**[†]

*MGMT promoter methylation status unavailable for 2 patients; [#]mean ± SD of original data. [†]Log-Rank test; RIC: relative invasiveness coefficient; MGMT: O-6-methylguanine-DNA methyltransferase; IDH-1: Isocitrate dehydrogenase 1; cm: centimeters; OS: overall survival; PFS: progression-free survival.

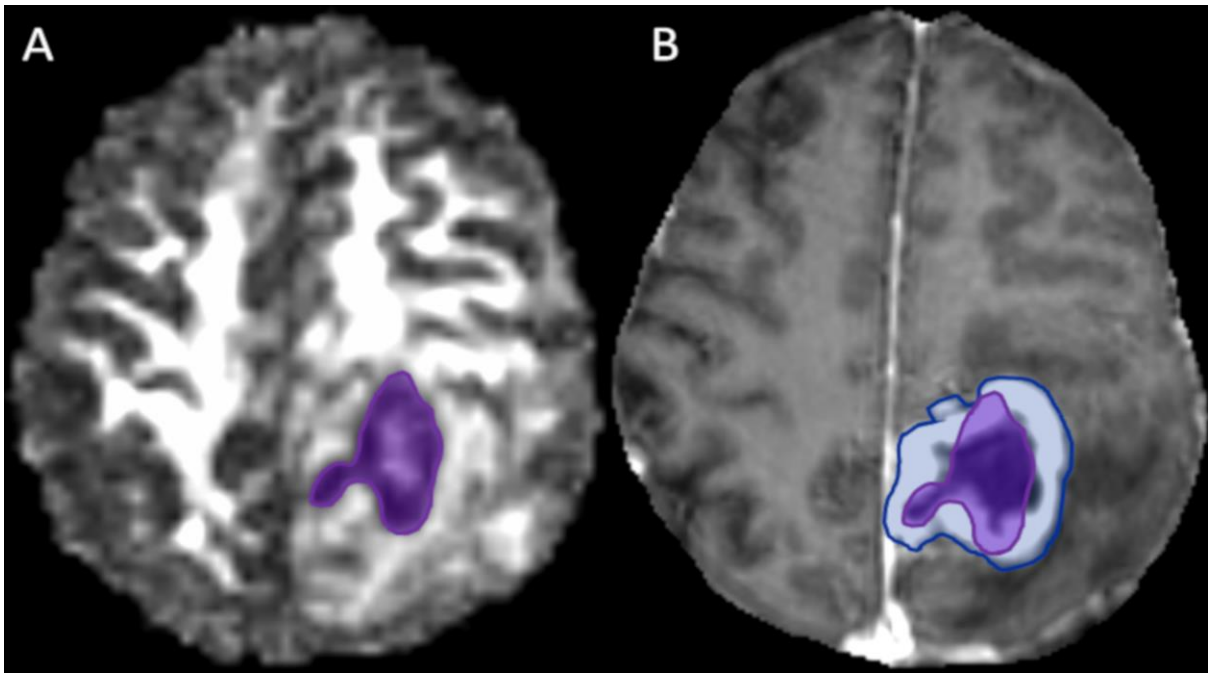
A
B

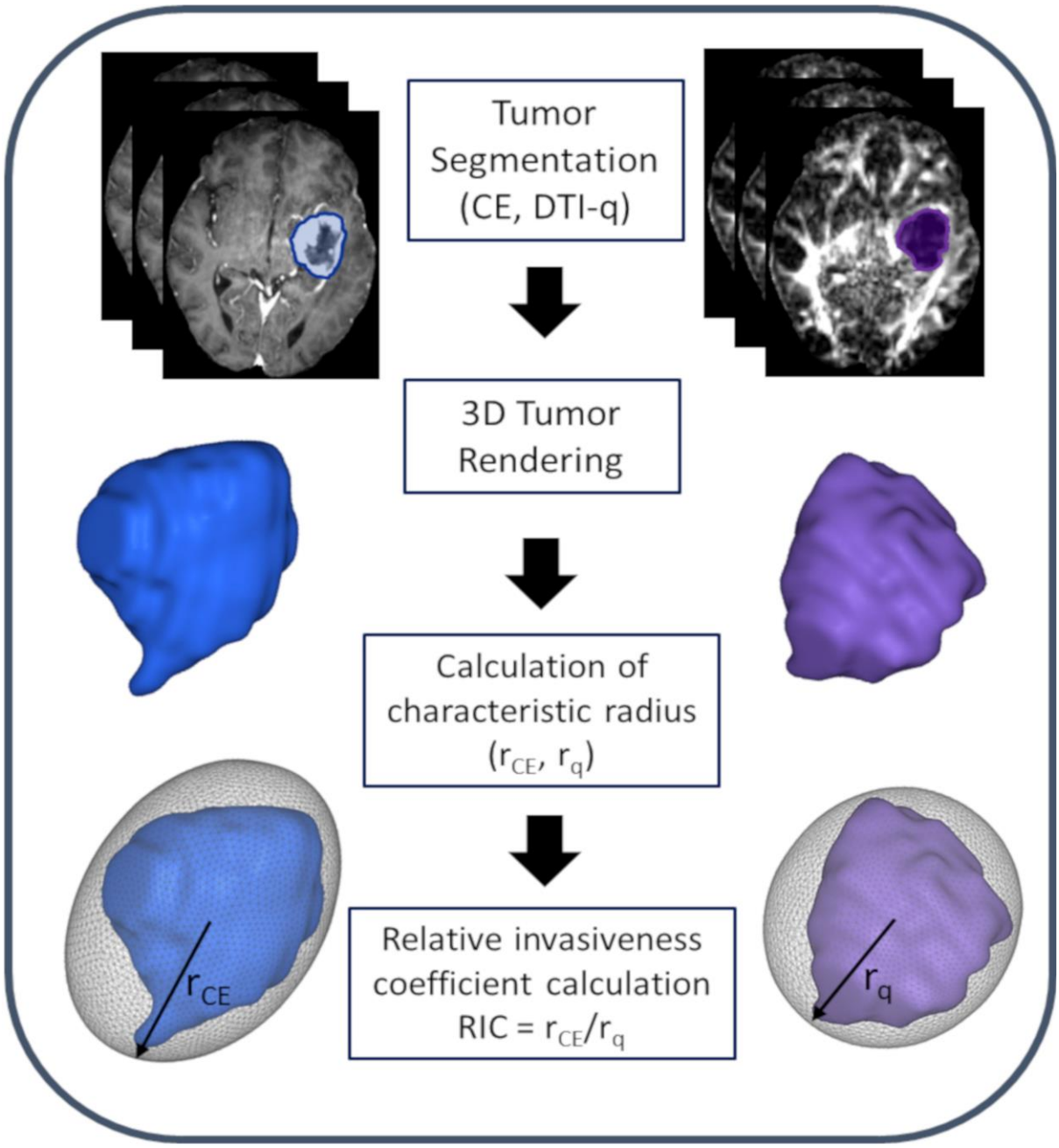
Tumor Segmentation (CE, DTI-q)
3D Tumor Rendering
Calculation of characteristic radius (r_{CE}, r_q)
Relative invasiveness coefficient calculation
RIC = r_{CE}/r_q
r_{CE}
r_q

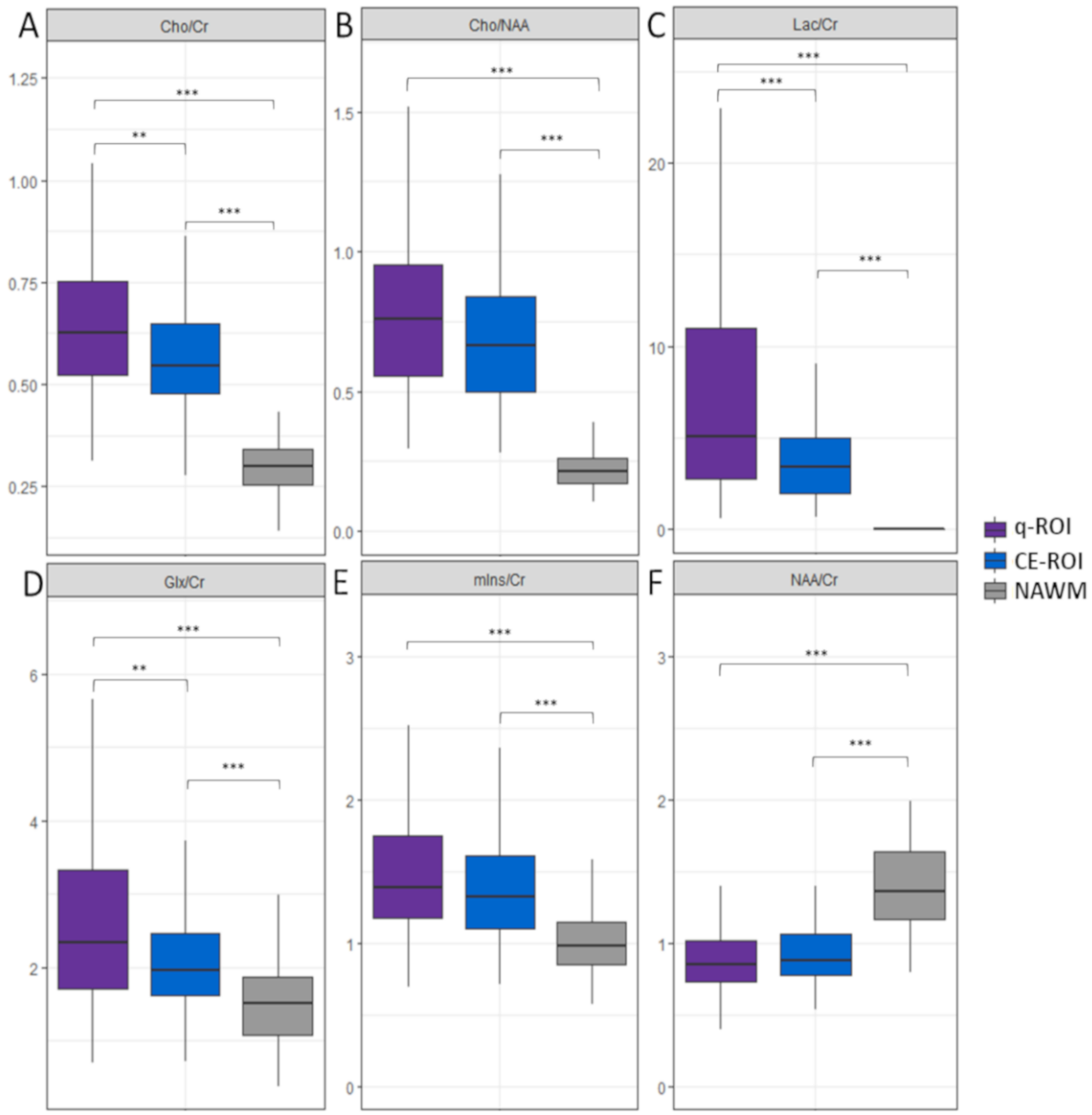
A
Cho/Cr
1.25
1.00
0.75
0.50
0.25
***
**
***
B
Cho/NAA
1.5
1.0
0.5
0.0
***
***
C
Lac/Cr
20
10
0
***
***
***
D
Glx/Cr
6
4
2
***
**
***
E
mIns/Cr
3
2
1
0
***
***
F
NAA/Cr
3
2
1
0
***
***
q-ROI
CE-ROI
NAWM

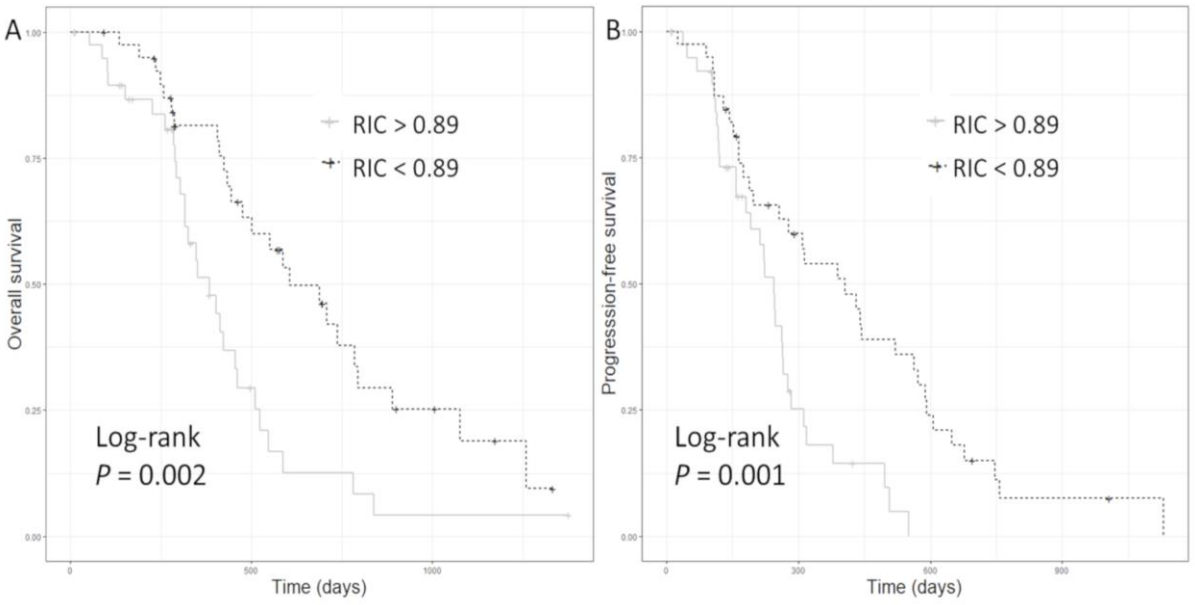
A
Overall survival
1.00
0.75
0.50
0.25
0.00
0
500
1000
Time (days)
RIC > 0.89
RIC < 0.89
Log-rank
P = 0.002
B
Progresssion-free survival
1.00
0.75
0.50
0.25
0.00
0
300
600
900
Time (days)
RIC > 0.89
RIC < 0.89
Log-rank
P = 0.001

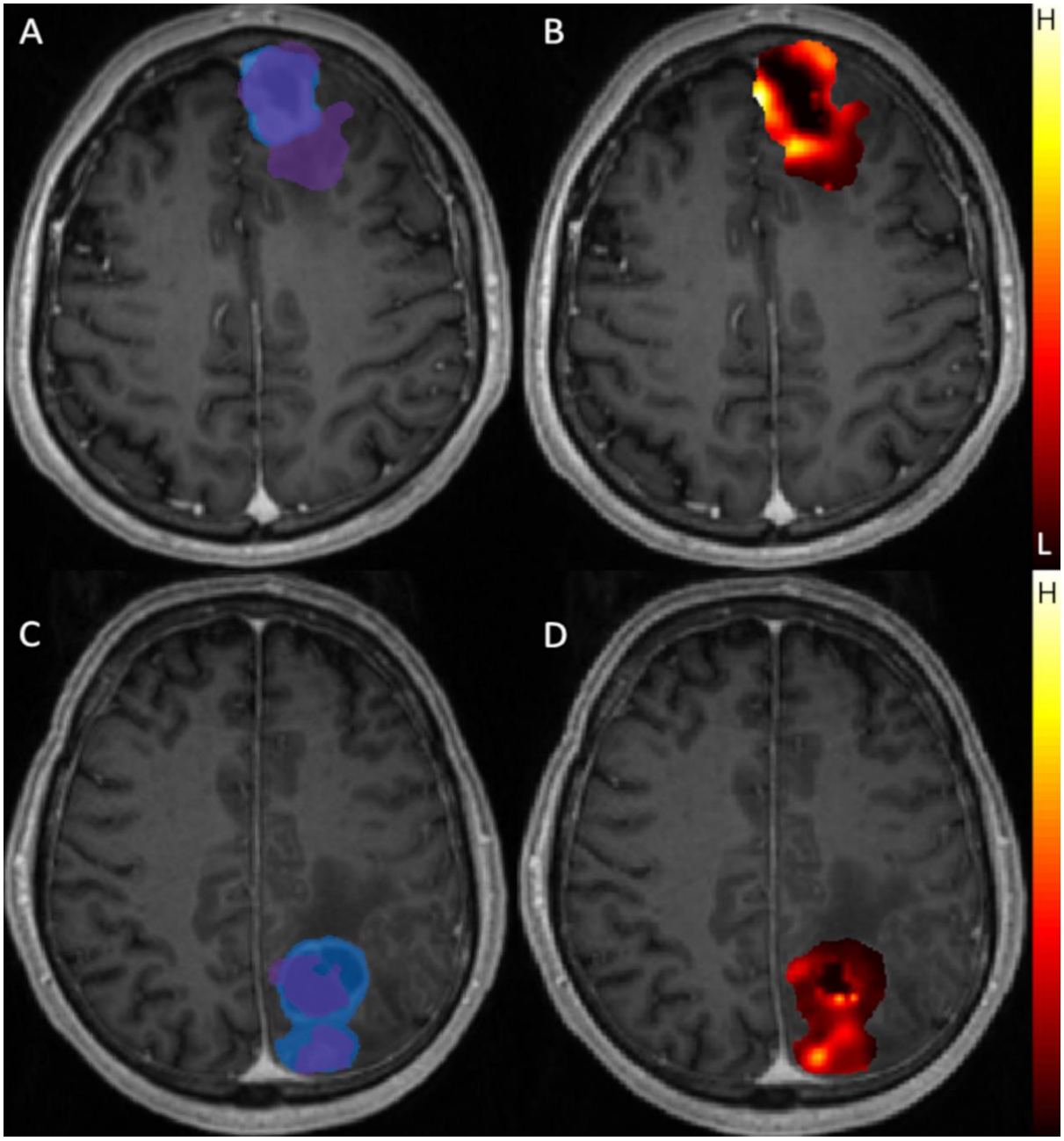
A
B
H
L
C
D
H

Figure legends

Figure 1. A demonstration of ROIs. A: DTI-q image; B: post-contrast T1-weighted image. The q-ROI (purple): the abnormality revealed on DTI-q map; CE-ROI (blue): the contrast-enhancing tumor region excluding DTI-q abnormality.

Figure 2. A demonstration of calculation of relative invasive coefficient. Tumor regsions are segmented from post-contrast T1 (left) and DTI-q images (right) respectively. The smallest ellipsoids are fitted to the tumor volume. The characteristic radii of ROIs (r_{CE}, r_q) are calculated as the semi-major axis of ellipsoids. A relative invasiveness coefficient (RIC) is calculated as the ratio of r_{CE}/r_q.

Figure 3. The metabolic signatures of ROIs. Both tumor ROIs display abnormal metabolic signatures. The q-ROI shows significantly higher levels of Cho/Cr, Lac/Cr, and Glx/Cr than CE-ROI. Cho: Choline; Cr: creatine; NAA: N-acetyl aspartate; Glx: glutamate + glutamine; mIns: myo-inositol; Lac: lactate; CE: contrast-enhancing. *: $P < 0.05$; **: $P < 0.01$; ***: $P < 0.001$.

Figure 4. Survivals of patient clusters. Log-rank test showed patients with a RIC > 0.89 displayed worse overall survival ($P = 0.002$) (A) and progression-free survival ($P = 0.001$) (B). RIC: relative invasiveness coefficient.

Figure 5. Two case examples of tumor invasiveness revealed by contrast enhancing tumor regions and DTI-q abnormalities. A&B: case 1 is a 64-year-old male, with a contrast enhancing tumor of 62.6 cm^3 and RIC of 0.81; C&D: case 2 is a 69-year-old male, with a contrast enhancing tumor of 31.2 cm^3 and RIC of 1.31. A&C indicate the CE-ROI (blue) and q-ROI (purple) in two patients. B&D indicate the rCBV maps on a voxel-wise basis across the CE-ROI and q-ROI. Both patients received tumor resection with the guidance of neuro-navigation and 5-aminolevulinic acid fluorescence for maximal resection. Complete resection was achieved in both patients according to the 72h post-operative MRIs. Pathological assessment confirmed both are MGMT promoter unmethylated and IDH-1 wild-type glioblastomas. Both patients received concomitant and adjuvant temozolomide chemoradiotherapy following Stupp protocol. The PFS and OS of case 1 were 563 and 697 days. The PFS and OS of case 2 were 159 and 317 days. RIC: relative invasiveness coefficient; CE: contrast enhancement; ROI: region of interest; PFS: progression-free survival; OS: overall survival.

References

1. Hegi ME, Diserens A, Gorlia T, et al. MGMT gene silencing and benefit from temozolomide in glioblastoma. *New Engl J Med* 2005;352:997-1003
2. Li YM, Suki D, Hess K, et al. The influence of maximum safe resection of glioblastoma on survival in 1229 patients: Can we do better than gross-total resection? *J Neurosurg* 2016;124:977-988
3. Stummer W, Meinel T, Ewelt C, et al. Prospective cohort study of radiotherapy with concomitant and adjuvant temozolomide chemotherapy for glioblastoma patients with no or minimal residual enhancing tumor load after surgery. *J Neuro-Oncol* 2012;108:89-97
4. Price SJ, Jena R, Burnet NG, et al. Improved delineation of glioma margins and regions of infiltration with the use of diffusion tensor imaging: An image-guided biopsy study. *Am J Neuroradiol* 2006;27:1969-1974
5. Wen PY, Macdonald DR, Reardon DA, et al. Updated Response Assessment Criteria for High-Grade Gliomas: Response Assessment in Neuro-Oncology Working Group. *Journal of Clinical Oncology* 2010;28:1963-1972
6. Price SJ, Gillard JH. Imaging biomarkers of brain tumour margin and tumour invasion. *Brit J Radiol* 2011;84:S159-S167
7. Sternberg EJ, Lipton ML, Burns J. Utility of Diffusion Tensor Imaging in Evaluation of the Peritumoral Region in Patients with Primary and Metastatic Brain Tumors. *Am J Neuroradiol* 2014;35:439-444
8. Potgieser ARE, Wagemakers M, van Hulzen ALJ, et al. The role of diffusion tensor imaging in brain tumor surgery: A review of the literature. *Clin Neurol Neurosur* 2014;124:51-58
9. Pena A, Green HAL, Carpenter TA, et al. Enhanced visualization and quantification of magnetic resonance diffusion tensor imaging using the p : q tensor decomposition. *Brit J Radiol* 2006;79:101-109
10. Li C, Wang S, Yan J-L, et al. Intratumoral Heterogeneity of Glioblastoma Infiltration Revealed by Joint Histogram Analysis of Diffusion Tensor Imaging. *Neurosurgery* 2018:nyy388-nyy388
11. Yan JL, van der Hoorn A, Larkin TJ, et al. Extent of resection of peritumoral diffusion tensor imaging-detected abnormality as a predictor of survival in adult glioblastoma patients. *Journal of Neurosurgery* 2017;126:234-241
12. Colwell N, Larion M, Giles AJ, et al. Hypoxia in the glioblastoma microenvironment: shaping the phenotype of cancer stem-like cells. *Neuro-Oncology* 2017;19:887-896
13. Kaur B, Khwaja FW, Severson EA, et al. Hypoxia and the hypoxia-inducible-factor pathway in glioma growth and angiogenesis. *Neuro Oncol* 2005;7:134-153
14. Vogelbaum MA, Jost S, Aghi MK, et al. Application of Novel Response/Progression Measures for Surgically Delivered Therapies for Gliomas: Response Assessment in Neuro-Oncology (RANO) Working Group. *Neurosurgery* 2012;70:234-243
15. Li C, Yan J-L, Torheim T, et al. Low Perfusion Compartments in Glioblastoma Quantified by Advanced Magnetic Resonance Imaging: Correlation with Patient Survival. *bioRxiv* 2017:180521
16. Smith SM, Jenkinson M, Woolrich MW, et al. Advances in functional and structural MR image analysis and implementation as FSL. *NeuroImage* 2004;23:S208-S219
17. Behrens TE, Woolrich MW, Jenkinson M, et al. Characterization and propagation of uncertainty in diffusion-weighted MR imaging. *Magn Reson Med* 2003;50:1077-1088
18. Moshtagh N. Minimum volume enclosing ellipsoid. *Convex Optimization* 2005;111:112
19. Kreis R. Issues of spectral quality in clinical H-1-magnetic resonance spectroscopy and a gallery of artifacts. *Nmr Biomed* 2004;17:361-381
20. Price SJ, Young AMH, Scotton WJ, et al. Multimodal MRI Can Identify Perfusion and Metabolic Changes in the Invasive Margin of Glioblastomas. *Journal of Magnetic Resonance Imaging* 2016;43:487-494

21. Mohsen LA, Shi V, Jena R, et al. Diffusion tensor invasive phenotypes can predict progression-free survival in glioblastomas. *Brit J Neurosurg* 2013;27:436-441
22. Price SJ, Jena R, Burnet NG, et al. Predicting patterns of glioma recurrence using diffusion tensor imaging. *European Radiology* 2007;17:1675-1684
23. Padhani AR, Miles KA. Multiparametric Imaging of Tumor Response to Therapy. *Radiology* 2010;256:348-364
24. Pardon MC, Lopez MY, Ding YC, et al. Magnetic Resonance Spectroscopy discriminates the response to microglial stimulation of wild type and Alzheimer's disease models. *Sci Rep-Uk* 2016;6
25. Noch E, Khalili K. Molecular mechanisms of necrosis in glioblastoma The role of glutamate excitotoxicity. *Cancer Biol Ther* 2009;8:1791-1797
26. Price SJ, Green HAL, Dean AF, et al. Correlation of MR Relative Cerebral Blood Volume Measurements with Cellular Density and Proliferation in High-Grade Gliomas: An Image-Guided Biopsy Study. *Am J Neuroradiol* 2011;32:501-506
27. Swanson KR, Rostomily RC, Alvord EC. A mathematical modelling tool for predicting survival of individual patients following resection of glioblastoma: a proof of principle. *British journal of cancer* 2008;98:113-119
28. Sanai N, Polley MY, McDermott MW, et al. An extent of resection threshold for newly diagnosed glioblastomas. *J Neurosurg* 2011;115:3-8
29. Stummer W, Pichlmeier U, Meinel T, et al. Fluorescence-guided surgery with 5-aminolevulinic acid for resection of malignant glioma: a randomised controlled multicentre phase III trial. *Lancet Oncol* 2006;7:392-401